Electronics and Communications in Japan, Part 1, Vol. 90, No. 1, 2007
Translated from Denshi Joho Tsushin Gakkai Ronbunshi, Vol. J89-B, No. 2, February 2006, pp. 115–125

Path Loss Prediction Model for the Over-Rooftop Propagation Environment of Microwave Band in Suburban Areas

Naoki Kita,[1] Wataru Yamada,[1] and Akio Sato[2]

[1]NTT Access Network Service Systems Laboratories, NTT Corporation, Yokosuka, 239-0847 Japan

[2]School of Computer Science, Tokyo University of Technology, Hachioji, 192-0982 Japan

SUMMARY

It is desirable that the method used for outdoor path loss estimation at microwave frequencies be one for which a worldwide consensus can be obtained through an ITU-R international standard. In this paper, a path loss prediction model for over-rooftop propagation environments is proposed for suburban areas. This model is based on the propagation mechanism explained by using the geometrical optics and consists of the direct wave region, the reflected wave region, and the diffracted wave region. The boundary points of these regions can be determined uniquely from the antenna height and building environment and all regions are continuously connected. Hence, high-precision estimation of the path loss can be estimated from the short-distance line-of-sight region to the far-field non-line-of-sight region. The proposed model is useful for channel design of microwave-band wireless access systems. Further, the method contributes to the ITU-R international standardization described above. Finally, it is shown that the measured path loss and the value estimated by the present model agree well at 2.2, 5.2, and 19.4 GHz. © 2006 Wiley Periodicals, Inc. Electron Comm Jpn Pt 1, 90(1): 13–24, 2007; Published online in Wiley InterScience (www.interscience.wiley.com). DOI 10.1002/ecja.20333

Key words: microwave band; over-rooftop propagation; path loss; geometrical optics; international standardization.

1. Introduction

The microwave frequencies centered around 5 GHz are a frequency range attracting worldwide attention for next-generation wireless communications. Mobile communications service is being shifted from the second generation, using 800-MHz and 1.5-GHz bands, to the third generation using 2-GHz and enabling broadband service. The holding of discussions on a fourth-generation mobile communications service with even faster speed has been considered. Wireless LAN systems such as IEEE802.11 have already achieved practical implementation. IEEE802.11b/g wireless systems using 2-GHz ISM (Industry Science Medical) band and indoor wireless LAN systems (IEEE802.11a) using the frequency range from 5.15 to 5.25 GHz have proliferated. Further, with regard to the 5-GHz band, the frequency range from 5.25 to 5.35 GHz (indoor communications and outdoor fixed communications) and the range from 5.47 to 5.725 GHz (outdoor use) were distributed by the WRC (World Radio Conference) to new wireless access systems in 2003. Domestic regularization is progressing. Under such conditions, radio propagation characteristics at microwave frequencies such as 5 GHz have been discussed. In particular, with regard to the path loss characteristics used as the basis for wireless zone design studies, an estimation model supported by an international consensus is desirable. Based on the above background, the ITU-R (International Telecommunications Union–Radiocommunications Sector) is drafting recommendations for various propagation characteristics and estimation methods in the microwave wireless access

environment and is planning to expand the applicable propagation environment and the applicable frequencies in the existing recommendations.

The recommendation with regard to a short-distance path loss estimation method is ITU-R Recommendation P.1411-2 [1]. In this recommendation, estimation methods of path loss for over-rooftop propagation environments are given in Section 4.2.1. This section is a recommendation based on the EURO-COST231 Walfisch–Ikegami model (W-I model) [2]. The applicable frequency range of the W-I model is limited to the interval between 800 MHz and 2 GHz, so that the estimation error at microwave frequencies is too large to be useful. With regard to ITU-R Recommendation P.1411, extension of the applicable upper frequency limit (from the 2-GHz band to the 5-GHz band) has been attempted by the method of aligning the coefficients of the estimation equation using measured data [3]. However, in the future, when extension to frequencies above 5 GHz is considered, the present method based on an estimation equation for the UHF band has limitations.

Studies on extending the applicable frequencies by various means have been carried out in addition to ITU-R Recommendation P.1411. They include studies of the path loss difference at microwave frequencies and UHF frequencies by measurement [4, 5], extension of the frequency term in the existing estimation equation by measured data regression [6], and the derivation of a microwave path loss empirical equation by the method of multiple regression [7]. There is no method that has worldwide acceptance. Further, if a method is used widely throughout the world, it is desirable that it provide high estimation accuracy with a site-general estimation method that does not require detailed geographical data.

In this paper, a path-loss model for over-rooftop propagation environments at microwave band considering the above concerns is proposed for suburban-zone microwave wireless Internet access service for individual users, public wireless LAN service, and next-generation mobile communications systems. The proposed path-loss model consists of three regions: the direct wave region, the reflected wave region, and the diffracted wave region. The method allows estimation of the path loss continuously from the short-distance line-of-sight region to the far-distance non-line-of-sight region.

The term "over-rooftop propagation" is used in this paper to mean radio propagation when the base station (BS) antenna is higher than the average building height in the target area and the mobile station (MS) antenna is lower than the average building height.

2. Boundary Point Model

In general, the path loss PL (dB) is known to increase in proportion to the logarithm of the distance d (m) between the BS and MS antennas. Whether indoors or outdoors, the following model is a simple path-loss model that has been widely studied in connection with international standardization such as ITU-R and IEEE802.11n [8]:

$$PL(d) = L_F(d_0) + N \cdot 10\log(d/d_0) + X_\sigma \quad (d \geq d_0)$$
$$L_F(d_0) = 20\log(4\pi d_0/\lambda) \tag{1}$$

Here d is the distance between the MS and BS antennas and N is the gradient of the path loss versus the logarithm of the distance between the MS and BS antennas. For free-space propagation, $N = 2$ is used. Also, X_σ (dB) is a random variable having a normal distribution with a mean of 0 and is a term expressing the variations of the median value of the short section. Further, d_0 (m) is the boundary point where the path-loss distance characteristic changes with respect to d. In Eq. (1), the gradient of the path loss versus d changes from 2 to N in Eq. (1) with d_0 as the boundary point. In this paper, a model such as the present one in which the path-loss characteristics change at a certain distance constituting the boundary point is called a "boundary point model." For d_0, approximate values are shown in Table 1 [8].

In this model, path-loss estimation equations for various propagation environments can be derived by letting the first term in Eq. (1) be constant and deriving the parameters N and X_σ from the measured data.

With regard to the parameters N and X_σ, studies have been performed for the suburban over-rooftop propagation environment [9, 10]. However, the model absorbs all of the variations of the path-loss characteristics due to the BS/MS antenna heights and other propagation environment factors into the parameters N and X_σ. Therefore, if modeling is performed for N and X_σ, the number of coefficient parameters with poor physical interpretations increases. The model becomes complex [9], cannot reflect the antenna height information [10], and provides poor estimation accuracy (when the value of X_σ becomes large) [8].

Figure 1 presents measured examples of path loss in a typical over-rooftop propagation environment. From the measured values, N is obtained by the least-squares method and Eq. (1) is derived. The results are shown in Fig. 1. From Table 1, d_0 is chosen as 100 m. From Fig. 1, it is found that

Table 1. Values of d_0 for Eq. (1)

Propagation environment	d_0
Urban microcell	1 km
Microcell	100 m
Indoor	1 m

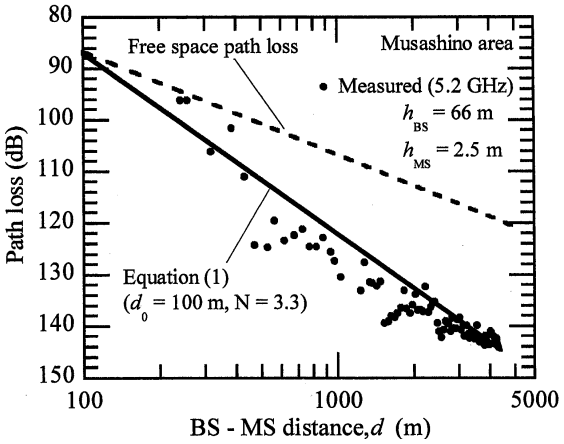

Fig. 1. Example of measured path loss in over-rooftop propagation environments in 5.2 GHz and calculated result by Eq. (1).

the numerical values given by Eq. (1) provide excessive values in the short-distance range and insufficiently large values at far distances.

In the subsequent sections of this paper, the propagation mechanism for the over-rooftop propagation environment is studied on the basis of the geometrical optics method. From the physical perspective, the boundary point where the path loss characteristics change is found. A path-loss model for the over-rooftop propagation environment reflecting these considerations is constructed.

3. Over-Rooftop Propagation Mechanism

Figure 2 shows a model of over-rooftop propagation based on geometrical optics (GO). A building environment is assumed to be homogeneous. In the figure, h_{BS}, h_{MS}, and $\langle h_1 \rangle$ are the BS antenna height, the MS antenna height, and the average building height in the area under consideration. Also, $\langle w \rangle$, w_1, and w_2 are the average building spacing in the area studied, the distance between the MS and the building on the BS side, and the distance between the MS and the building on the other side of the BS. In the upper scale in Fig. 2, ϕ is the angle between the straight line connecting the BS and MS antennas and the building edge (building angle). As multiple waves, the normal reflected wave and the once-diffracted wave from the building roof, for which the arrival level at the MS is considered high, are indicated.

From Fig. 2, it is found that the configuration of the multiple waves arriving at the MS depends on the distance between the BS and MS antennas. The region in which the direct wave can arrive at the MS is limited to a small region with a short line-of-sight distance between the BS and MS antennas. The reflected wave in this region may be neglected because it is smaller in relative terms than the direct

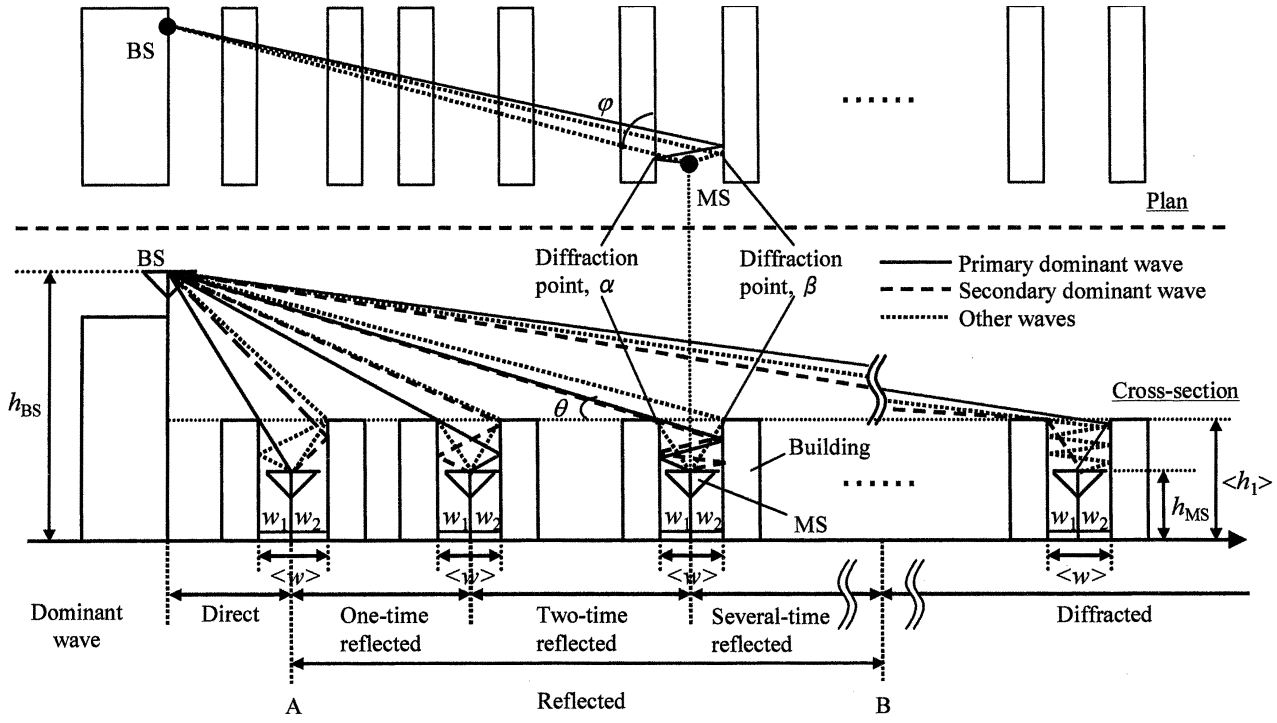

Fig. 2. Propagation model for over rooftops based on geometrical optics.

wave. The path loss is close to that in free space. In regions farther away, the wave diffracted from rooftops and the wave reflected from the walls of buildings become dominant. In such regions, the path loss is governed by whichever of the reflected wave and the diffracted wave arriving at the MS has a larger arrival level.

When the distance between the BS and MS antennas is small and the elevation angle (θ in Fig. 2) looking at the BS antenna from the building edge on the BS side of the specific MS is rather large, reflected waves with a relatively low number of reflections (1 to 3 times) arrive at the MS. On the other hand, if the distance between the BS and MS antennas is large and θ is small, only reflected waves with small arrival levels after many reflections arrive. With regard to the effects of variations of the multiple wave configuration arriving at the MS on the path loss, measurement of the received levels and simulation of ray tracing are performed. For the ray tracing simulation, the direct wave, normal reflected waves with 1 to 8 reflections, and once-diffracted waves from two building roofs before and after the MS, are taken into account. For simplicity, only two buildings before and after the MS are considered, and they are approximated as rectangular bodies. For calculations of the diffracted waves, the UTD (Uniform Theory of Diffraction) [11] for metal edges is used. For calculations of the reflection coefficients on the wall surfaces of the buildings, a complex permittivity of 6.95–*j*0.74 (that of concrete at 5 GHz) [12] is used. The measurement environment is a residential area in Tokyo (Suginami Ward). Apartment buildings of 3 to 5 floors are interspersed among houses with 2 floors. The ground is flat and the average height of the buildings in the measurement area $\langle h_1 \rangle$ is about 8.5 m.

The characteristics of multipath waves in an over-rooftop propagation environment can easily be understood if the height characteristics of the MS antenna for the arriving wave (height pattern characteristics) are considered. Both the calculated and measured results are normalized by letting the average level of the received power in the LOS (Line-Of-Sight) region on the building roofs above about 2 m be 0 dB. Figure 3(a) shows the results for when the BS–MS distance is rather short and θ = 4.06°, and Fig. 3(b) shows those for rather long BS–MS distances and θ = 0.94°. The measured values are averages of the power over a 1-m section in the height direction.

In Figs. 3(a) and 3(b), the numerical results and the measured results agree well. The simulation results also indicate the contents of the arriving multipath waves. In the figure, (0) denotes the direct wave, (1) to (3) the 1- to 3-time reflected waves, and (D) the once-diffracted wave. Although the once-diffracted waves arrive at any height, there are restrictions on the height for the direct wave and the reflected waves. The lengths of the straight lines for (0) to (3) indicate the height ranges in which the respective wave can be received. It is found that the distance variation is

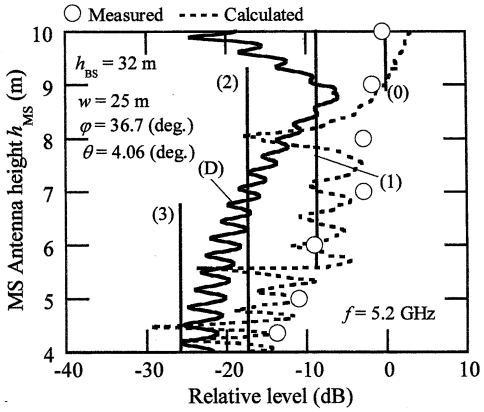

(a) When BS-MS distance is relatively short (d = 330 m)

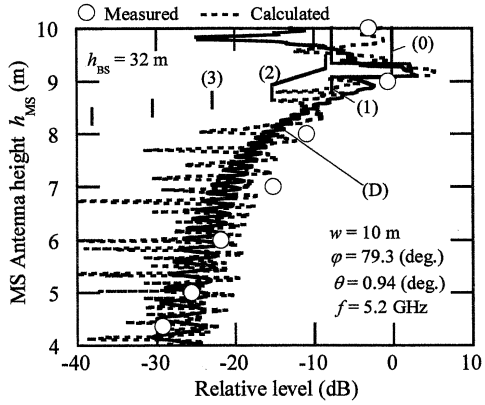

(b) When BS-MS distance is relatively long (d = 1360 m)
(0) Direct wave, (1) 1-time reflected wave, (2) 2-time reflected wave, (3) 3-time reflected wave, (D) 1-time diffracted wave

Fig. 3. Example of characteristics of multipath waves in over-rooftop propagation environment.

small for the direct wave level in the range and that the reflected wave levels are almost constant because the angle-of-incidence variations in the range are small.

In Fig. 3(a), the 1- to 2-time reflected waves arrive in the low antenna height region (where the MS is located) and are dominant over the entire level (power derived from the vector sum of the direct, reflected, and diffracted waves). Hence, the entire level decays from the high antenna height region to the low antenna height region in the order of the MS levels for which the direct wave, once-reflected wave, and twice-reflected wave can arrive. On the other hand, in Fig. 3(b), the once-diffracted wave becomes dominant as the reflected waves with several reflections cannot arrive at the low antenna height region where the MS is located. Hence, the entire level varies according to the once-diffracted wave level.

As shown in the lower part of Fig. 2, the over-rooftop path loss can be divided into the following three regions depending on the arriving wave dominant to the entire level:

① the direct wave region where the direct wave arrives at the MS, ② the reflected wave region in which reflected waves with a few reflections arrive, and ③ the diffracted wave region in which the diffracted waves are dominant. A path-loss estimation equation can be obtained by modeling the path-loss characteristics in these three regions and the two boundary points separating these three regions.

4. Over-Rooftop Path-Loss Model

In this paper, with a view to constructing a path-loss estimation method that is general with respect to sites, we attempt to estimate the average of the median value of the path loss in short sections. Hence, the central values in each parameter range are chosen with regard to the street angle ϕ, the distance w_1 between the MS and the building on the BS side, and the distance w_2 between the MS and the building on the other side of the BS. Here $\phi = 45°$ and $w_1 = w_2 = 1/2 \langle w \rangle$. In the following mathematical derivations, ϕ, w_1, and w_2 are used in order to preserve the physical meaning of the equations.

Also, the present model assumes a rather homogeneous propagation environment such as a residential area where the building height and the building spacing are uniform.

4.1. Path loss model in three regions

4.1.1. Direct wave region

The path loss $L_F(d)$ in the direct wave region can be approximated by the free space loss, since the direct wave is dominant over the other contributions. If the BS–MS antenna distance is d, then

$$L_F(d) \approx 20 \cdot \log\left(\frac{4\pi d}{\lambda}\right) \quad (d \in \text{direct wave region}) \tag{2}$$

4.1.2. Reflected wave region

In the region where the reflected waves are dominant, the path loss is close to the loss value of the k-fold-reflected wave at the arrival distance limit of the k-fold-reflected wave as shown in Fig. 3(a). If the BS–MS antenna distance is d_k when the k-fold-reflected wave reaches the arrival limit, and if the propagation path length of the k-fold-reflected wave is d_{kp}, the path loss L_{d_k} at the arrival limit of the k-fold-reflected wave is given by

$$L_{d_k} \approx 20 \cdot \log\left\{\frac{4\pi d_{kp}}{\lambda \cdot R^k}\right\} \quad (d_k \in \text{reflected wave region}) \tag{3}$$

Here R is the reflection coefficient of the wall surface of the building at microwave frequencies and is specified as –8 dB with reference to Ref. 13. Also, in terms of the variables in Fig. 2, d_{kp} and d_k are geometrically given by

$$d_{kp} = \frac{1}{\sin\varphi_k} \cdot \sqrt{{A_k}^2 + (h_{BS} - h_{MS})^2} \tag{4a}$$

$$d_k = \frac{1}{\sin\varphi} \cdot \sqrt{{B_k}^2 + (h_{BS} - h_{MS})^2} \tag{4b}$$

Here,

$$A_k = \begin{cases} \dfrac{h_{BS} - h_{MS}}{\langle h_1 \rangle - h_{MS}} \cdot (k \cdot \langle w \rangle + w_1) & (k\text{: Even}) \\ \dfrac{h_{BS} - h_{MS}}{\langle h_1 \rangle - h_{MS}} \cdot (k \cdot \langle w \rangle + w_2) & (k\text{: Odd}) \end{cases}$$
$$(k = 0, 1, 2, \cdots)$$

$$B_k = \begin{cases} \dfrac{h_{BS} - h_{MS}}{\langle h_1 \rangle - h_{MS}} \cdot (k \cdot \langle w \rangle + w_1) - k \cdot \langle w \rangle & (k\text{: Even}) \\ \dfrac{h_{BS} - h_{MS}}{\langle h_1 \rangle - h_{MS}} \cdot (k \cdot \langle w \rangle + w_2) - 2w_2 - (k-1) \cdot \langle w \rangle & (k\text{: Odd}) \end{cases}$$
$$(k = 0, 1, 2, \cdots)$$

$$\varphi_k = \tan^{-1}\left(\frac{B_k}{A_k} \cdot \tan\varphi\right)$$

Also, the path loss between the limiting point of the k-fold-reflected wave and that of the k + 1-fold-reflected wave is found to be subject to linear interpolation by Fig. 3(a). Hence, the path loss in the reflected wave region can be given by the following, obtained from linear interpolation with Eq. (3):

$$L_R(d) = L_{d_k} + \frac{L_{d_{k+1}} - L_{d_k}}{d_{k+1} - d_k} \cdot (d - d_k)$$
$$(k = 0, 1, 2, \cdots)$$
$$(d \in \text{reflected wave region}) \tag{5}$$

4.1.3. Diffracted wave region

In the diffracted wave region, the arriving wave that is dominant in the path loss is the once-diffracted wave from the building edge as shown in Fig. 3(b). As the once-diffracted wave, let us consider the diffracted wave from the diffraction points α and β in Fig. 2. Hence, the path loss $L_D(d)$ in the diffracted wave region is as follows:

$$L_D(d) \approx -10 \cdot \log\left\{\left(\frac{\lambda \cdot D_\alpha}{4\pi d_{a,\alpha}\sqrt{d_{b,\alpha}}}\right)^2 + \left(\frac{\lambda \cdot D_\beta}{4\pi d_{a,\beta}\sqrt{d_{b,\beta}}}\right)^2\right\} \tag{6}$$

where D_α and D_β are the UTD diffraction coefficients. Although the UTD diffraction coefficient has polarization dependence, the diffraction coefficients used here are the averages of the results for vertical and horizontal polarizations. Here $d_{a,\alpha}$ and $d_{a,\beta}$ are the distances from the BS antenna to diffraction points α and β, while $d_{b,\alpha}$ and $d_{b,\beta}$ are the distances from diffraction points α and β to the MS. These are given by

$$d_{a,\alpha} = \sqrt{\left\{\sqrt{d^2-(h_{BS}-h_{MS})^2} - \frac{w_1}{\sin\varphi}\right\}^2 + (h_{BS}-\langle h_1\rangle)^2}$$

$$d_{b,\alpha} = \sqrt{\left(\frac{w_1}{\sin\varphi}\right)^2 + (\langle h_1\rangle - h_{MS})^2}$$

$$d_{a,\beta} = \sqrt{\left\{\sqrt{d^2-(h_{BS}-h_{MS})^2} + \frac{w_2}{\sin\varphi_k}\right\}^2 + (h_{BS}-\langle h_1\rangle)^2}$$

$$d_{b,\beta} = \sqrt{\left(\frac{w_2}{\sin\varphi_k}\right)^2 + (\langle h_1\rangle - h_{MS})^2}$$

($d \in$ diffracted wave region)

In Eq. (6), when only the BS–MS antenna distance d varies, $d_{b,\alpha}$ and $d_{b,\beta}$ do not change: only $d_{a,\alpha}$ and $d_{a,\beta}$ change linearly with d. In the diffracted wave region in which the BS–MS antenna distance is rather large, the distance characteristics of the path loss depend only only on those of the path loss between the diffraction points on the roof and the BS antenna. Hence, the distance characteristics of the path loss are in agreement with the slope of the free space characteristics.

However, we know that, in general in the NLOS (Non-Line-Of-Sight) environment, the slope of the path loss is $N > 2$. This is believed be affected by path blockage between the BS antenna and the diffraction point and by Fresnel zone shielding [14]. In the present paper, the value of N is derived by measured results in the diffracted wave region with a rather large BS–MS antenna distance d.

Let us modify Eq. (6) into the following form and apply the least-squares method to the measured values in order to derive N:

$$L_D(d) = N \cdot 10\log(d) + C \quad (d \in \text{diffracted wave region}) \tag{7}$$

where C is a constant.

The present authors have already found N experimentally in the diffracted wave region. Measurements were performed in two different suburban environments. The path-loss measurements were carried out at 2.2 and 5.2 GHz [4]. The results are shown in Table 2. There is no significant difference in N between 2.2 and 5.2 GHz. Although the results have some fluctuations depending on the antenna height conditions, there is no clear dependence of N on the base station antenna height. The value of N is 2.7 (2.2 GHz) in the smallest case and 3.7 (5.2 GHz) in the largest case. The average value of N for 12 measurements is 3.25, which is used in the model. And this value is also close to the measured result (N = 3.12) at 3.7 GHz in the suburban area as found by another organization [10].

Table 2. Slope of path loss N for propagation distance

Area	h_{BS} (m)	h_{MS} (m)	N (2.2GHz)	N (5.2GHz)	ID
Yokosuka	13	2.8	3.2	3.1	①
Suginami	18	2.8	2.7	3.0	②
		3.8	3.6	3.7	③
	21	3.8	3.4	3.4	④
	32	2.8	3.1	2.9	⑤
		3.8	3.5	3.4	⑥

Hence, the path loss $L_D(d)$ in the diffracted wave region is

$$L_D(d) = 3.25 \cdot 10\log(d) + C \tag{8a}$$

Let d_{RD} be the BS–MS antenna distance at the boundary point between the reflected wave region and the diffracted wave region, and let $L_{d_{RD}}$ be the corresponding path loss. Since the path loss is continuous at the boundary point, C is given by

$$C = L_{d_{RD}} - 32.5\log(d_{RD}) \tag{8b}$$

Therefore, from Eqs. (8a) and (8b), $L_D(d)$ is given by

$$L_D(d) = 32.5\log\left(\frac{d}{d_{RD}}\right) + L_{d_{RD}} \quad (d \in \text{diffracted wave region}) \tag{8c}$$

4.2. Boundary points between regions

The boundary points between the direct wave region and the reflected wave region and between the reflected wave region and the diffracted wave region can be obtained as the arrival limit distances of the direct wave and the distance at which the reflected wave loss arriving at the MS is equal to the diffracted wave loss arriving at the MS. In this section, the boundary points and the path loss at the boundary points are discussed.

4.2.1. Boundary point between the direct wave region and the reflected wave region

The BS–MS antenna distance d_0 at the boundary point (point A in Fig. 2) can be derived geometrically as follows, by using the variables shown in Fig. 2:

$$d_0 = \frac{h_{BS} - h_{MS}}{\langle h_1 \rangle - h_{MS}} \cdot \frac{1}{\sin\varphi} \cdot \sqrt{{w_1}^2 + (\langle h_1 \rangle - h_{MS})^2} \tag{9a}$$

Then the path loss $L_f(d_0)$ is expressed as

$$L_f(d_0) \approx 20 \cdot \log(4\pi d_0/\lambda) \tag{9b}$$

where λ is the wavelength.

4.2.2. Boundary point between the reflected wave region and the diffracted wave region

The BS–MS antenna distance d_{RD} at the boundary point (point B in Fig. 2) is the value of d at which $L_R(d)$ represented by Eq. (5) is equal to $L_D(d)$ represented by Eq. (6). However, since Eq. (6) contains the UTD diffraction coefficient, it is difficult to derive the solution analytically and easily. Therefore, the solution is sought by computer numerical calculations. However, to allow the construction of a simple estimation method, a method for deriving d_{RD} approximately is described.

Figure 4 presents numerical examples for $L_R(d)$ and $L_D(d)$ at 2, 5, 8, 15, and 30 GHz. The average building height $\langle h_1 \rangle$ and the average building width $\langle w \rangle$ used in the calculations are those typical in suburban areas [3]. The numerical results are normalized to the direct wave level at which d equals d_0, taken as 0 dB. The building reflection coefficient R is considered approximately constant at microwave frequencies on the basis of experimental investigations [13]. When normalization is used with the direct wave level at d_0 as 0 dB, $L_R(d)$ does not have frequency dependence. On the other hand, since the diffraction coefficient is frequency dependent, $L_D(d)$ provides different values at different frequencies. Hence, d_{RD} obtained as the reading of the horizontal axis at the intersection of $L_R(d)$ and $L_D(d)$ in Fig. 4 is different at each frequency.

Let us consider replacing the true d_{RD} at each frequency by d_k, which can easily be derived geometrically. In Fig. 4, d_k with the closest value to d_{RD} is alternatively chosen as d_{RD}, while $d_{RD} \approx d_k$ in the case

$$\frac{d_{k-1} + d_k}{2} < d_{RD} \leq \frac{d_k + d_{k+1}}{2} \tag{10}$$

Hence, from Fig. 4,

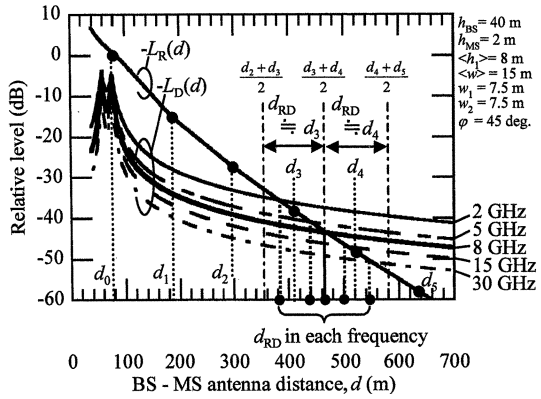

Fig. 4. Boundary between reflected and diffracted dominant regions.

$$d_{RD} \approx \begin{cases} d_3 & (f \leq 8\,\text{GHz}) \\ d_4 & (f > 8\,\text{GHz}) \end{cases} \tag{11a}$$

at microwave frequencies. Thus, the path loss $L_{d_{RD}}$ can be expressed from Eqs. (5), (11a), and (3) as follows:

$$L_{d_{RD}} = \begin{cases} L_{d_3} = 20 \cdot \log\left\{\dfrac{4\pi d_{3p}}{\lambda \cdot R^3}\right\} & (f \leq 8\,\text{GHz}) \\ L_{d_4} = 20 \cdot \log\left\{\dfrac{4\pi d_{4p}}{\lambda \cdot R^4}\right\} & (f > 8\,\text{GHz}) \end{cases} \tag{11b}$$

Here d_{RD}, d_3, and d_4 have a dependence on the average building spacing $\langle w \rangle$, the average building height $\langle h_1 \rangle$, the BS antenna height h_{BS}, and the MS antenna height h_{MS}. In particular, for h_{BS} and h_{MS}, the difference from the average building height $\langle h_1 \rangle$ affects d_{RD}, d_3, and d_4.

4.3. Recommended parameter range of the present estimation method

In this section, the estimated value errors are described by letting $d_{RD} \approx d_3$ at $f < 8$ GHz and $d_{RD} \approx d_4$ at $f >$ 8 GHz. The recommended ranges of the parameters used in the present path-loss estimation method are also described.

The path-loss estimation error $|\varepsilon|$ in the diffracted wave region resulting from the replacement of d_{RD} by d_3 at frequencies higher than 2 GHz but lower than 8 GHz is given by the following, based on Eq. (8c):

$$\varepsilon = 32.5 \log(d_3/d_{RD}) \quad (\text{dB}) \tag{12}$$

Δh_{B1} and Δh_{1M} are defined as follows:

$$\Delta h_{B1} \equiv h_{BS} - \langle h_1 \rangle \tag{13a}$$

$$\Delta h_{1M} \equiv \langle h_1 \rangle - h_{MS} \tag{13b}$$

Figure 5 shows the |ε| characteristics versus Δh_{B1}. The frequency f is targeted at 2 GHz, the lower limit of the frequencies considered, and 8 GHz, the upper limit with $d_{RD} \approx d_3$. In the calculations, Δh_{1M} is used as a parameter. Here, <w> = 15 m is used.

From Fig. 5, it is found that |ε| is less than about 3 dB in the following ranges:

$$2\,\mathrm{GHz} < f \leq 8\,\mathrm{GHz} \quad (d_{RD} \fallingdotseq d_3) \tag{14a}$$

$$\Delta h_{B1} \leq 100\,\mathrm{m} \tag{14b}$$

$$4\,\mathrm{m} \leq \Delta h_{1M} \leq 10\,\mathrm{m} \tag{14c}$$

Further, the <w> dependence of ε is derived for a large |ε| ① (Δh_{1m} = 4 m, f = 2 GHz) and ② (Δh_{1m} = 10 m, f = 8 GHz). The following range of <w> is considered typical in suburban areas [3]:

$$10\,\mathrm{m} \leq \langle w \rangle \leq 25\,\mathrm{m} \tag{14d}$$

Figure 6 shows the results. In Fig. 6, ① and ② correspond to ① and ② in Fig. 5. In the case of ① |ε| is about 4 dB if <w> = 25 m. If <w> < 20 m, |ε| is almost always less than 3 dB except for Δh_{B1} < 20 m. Even for the case of Δh_{B1} < 20 m, the maximum |ε| is about 5 dB. In the case of ② the value of |ε| is less than 3 dB except for <w> = 10 m. Even for the case of <w> = 10 m, it is found that the value of |ε| is kept below 4 dB in the region of Δh_{B1} < 100 m.

The above discussion is similarly repeated at different frequencies, such as 8 GHz, the lower limit of $d_{RD} \approx d_4$,

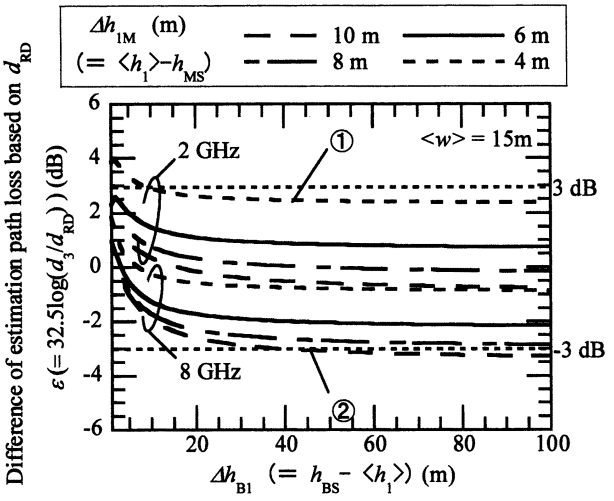

Fig. 5. Dependency of ε on Δh_{1M}.

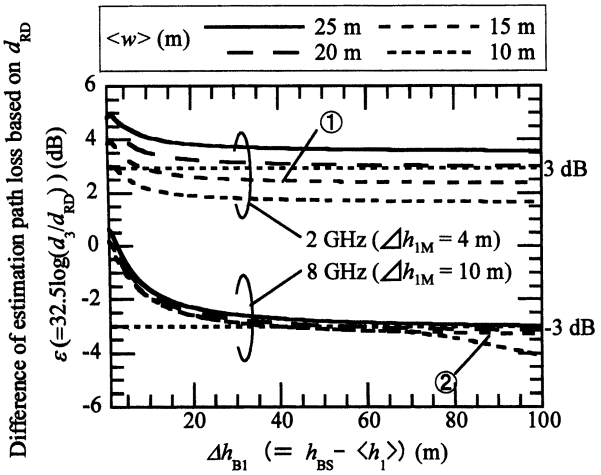

Fig. 6. Dependency of ε on <w>.

and 30 GHz, the upper limit of microwave frequencies, and similar results are obtained.

Hence, the parameter ranges where |ε| is less than about 3 dB [(14a) to (14d)] are the recommended ones.

4.4. Model expression

The discussion is now summarized by model representations.

[Direct wave region] ($d \leq d_0$)

$$L(d) = 20 \cdot \log\left(\frac{4\pi d}{\lambda}\right) \tag{15a}$$

[Reflected wave region] ($d_0 < d \leq d_m$)

$$m = \begin{cases} 3 & (f \leq 8\,\mathrm{GHz}) \\ 4 & (f > 8\,\mathrm{GHz}) \end{cases}$$

For $d_k < d \leq d_{k+1}$,

$$L(d) = L_{d_k} + \frac{L_{d_{k+1}} - L_{d_k}}{d_{k+1} - d_k} \cdot (d - d_k) \tag{15b}$$
$$(k = 0, \cdots, m-1)$$

[Diffracted wave region] ($d_m < d$)

$$m = \begin{cases} 3 & (f \leq 8\,\mathrm{GHz}) \\ 4 & (f > 8\,\mathrm{GHz}) \end{cases}$$

$$L(d) = 32.5 \log(d/d_m) + L_{d_m} \tag{15c}$$

where

$$d_k = \frac{1}{\sin\varphi} \cdot \sqrt{B_k{}^2 + (h_{BS} - h_{MS})^2} \tag{16a}$$

$$L_{d_k} = 20 \cdot \log \left\{ \frac{4\pi d_{kp}}{\lambda \cdot R^k} \right\} \quad (16b)$$

$$d_{kp} = \frac{1}{\sin \varphi_k} \cdot \sqrt{{A_k}^2 + (h_{BS} - h_{MS})^2} \quad (16c)$$

$$A_k = \begin{cases} \dfrac{h_{BS} - h_{MS}}{\langle h_1 \rangle - h_{MS}} \cdot (k \cdot \langle w \rangle + w_1) & (k\text{: Even}) \\ \dfrac{h_{BS} - h_{MS}}{\langle h_1 \rangle - h_{MS}} \cdot (k \cdot \langle w \rangle + w_2) & (k\text{: Odd}) \end{cases} \quad (16d)$$

$$B_k = \begin{cases} \dfrac{h_{BS} - h_{MS}}{\langle h_1 \rangle - h_{MS}} \cdot (k \cdot \langle w \rangle + w_1) - k \cdot \langle w \rangle & (k\text{: Even}) \\ \dfrac{h_{BS} - h_{MS}}{\langle h_1 \rangle - h_{MS}} \cdot (k \cdot \langle w \rangle + w_2) - 2w_2 - (k-1) \cdot \langle w \rangle & (k\text{: Odd}) \end{cases} \quad (16e)$$

$$\varphi_k = \tan^{-1} \left(\frac{B_k}{A_k} \cdot \tan \varphi \right) \quad (16f)$$

$$R = 10^{-8/20} \quad (16g)$$

4.5. Computational method

4.5.1. Parameters needed for calculations

The parameters needed for the calculations are listed in Table 3, including the recommended ranges.

In this paper, from the point of view of constructing a site-general path-loss estimation equation, the building angle ϕ, the spacing w_1 between the MS and the building on the BS side, and the spacing w_2 between the MS and the building on the opposite side of the BS, are such that $\phi = 45°$, $w_1 = w_2 = 1/2 \langle w \rangle$.

Specifically, if a value other than 45° is used for ϕ, the error $|\varepsilon|$ defined in Section 4.3 becomes greater than 3 to 4 dB if ϕ is less than 10°. Hence, if the estimation equation is used with ϕ as a parameter, it is desirable to use the following range:

$$10° < \varphi \leq 90° \quad (17)$$

4.5.2. Computational procedure

With the calculation of the path loss versus BS–MS antenna distance d as an example, the computational method is presented below.

(1) The frequency f for calculation of the path loss is determined.

(2)
- (For $f \leq 8$ GHz), d_0, d_1, d_2, and d_3 are derived from Eqs. (16a) and (16b).
- (For $f > 8$ GHz), d_4 is derived in addition to d_0, d_1, d_2, and d_3.

(3) The initial value of d is determined.

(4)
- If $d \leq d_0$, the path loss is calculated from Eq. (15a).
- If $d_0 < d \leq d_1$, the path loss is calculated with $k = 0$ in Eq. (15b).
- If $d_1 < d \leq d_2$, the path loss is calculated with $k = 1$ in Eq. (15b).
- If $d_2 < d \leq d_3$, the path loss is calculated with $k = 2$ in Eq. (15b).
- (For $f > 8$ GHz), if $d_3 < d \leq d_4$, the path loss is calculated with $k = 3$ in Eq. (15b).
- (For $f \leq 8$ GHz), if $d_3 < d$, the path loss is calculated with $m = 3$ in Eq. (15c).
- (For $f > 8$ GHz), if $d_4 < d$, the path loss is calculated with $m = 4$ in Eq. (15c).

(5) Update d.

(6) Iterate steps (4) and (5).

Numerical examples are given in Fig. 7.

Table 3. Parameters for calculations

	Parameters	Recommended range
$\langle h_1 \rangle$	Average building height (m)	$< h_{BS}$
$\langle w \rangle$	Average building spacing (m)	10–25 m
f	Frequency (GHz)	2.2–19.4 GHz (range verified in the next section)
d	BS–MS antenna spacing (m)	< 5000 m (range verified in the next section)
h_{BS}	BS antenna height (m)	$\langle h_1 \rangle$ to $\langle h_1 \rangle$ + 100 m
h_{MS}	MS antenna height (m)	$\langle h_1 \rangle$ –10 to $\langle h_1 \rangle$ –4 m

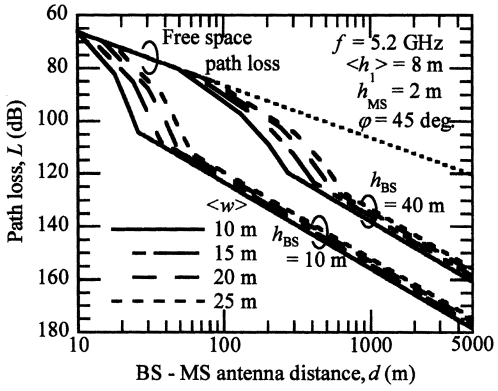

Fig. 7. Examples of calculation results.

Table 4. Measurement scenarios

	h_{BS}	h_{MS}	$<w>$	$<h_1>$	Freq.
Setagaya	37 m	3.0 m	15 m	8.5 m	2.2, 5.2 GHz
Musashino	66 m	2.5 m	12 m	8.0 m	2.2, 5.2, 19.4 GHz

5. Comparison with Measured Data

5.1. Measurement environment

The path loss is measured at 2.2, 5.2, and 19.4 GHz. A 90° directive antenna in the horizontal plane and an omnidirectional antenna in the horizontal plane are used as the BS and MS antennas, respectively. The polarization is vertical. For verification of the estimation method, the measurement locations were two other than those in Table 2. Table 4 shows the measurement scenarios.

Setagaya District and Musashino District, chosen for measurement, have rather homogeneous propagation environments with typical residential areas.

5.2. Comparison with computational values

From the measured results, the average of the median value of the path loss in short sections is calculated and compared with the computational results. The results are presented in Figs. 8 and 9.

In Fig. 8, the computational and measured results agree for both 2.2 and 5.2 GHz. In Fig. 9, the difference between the computational results and the measured results

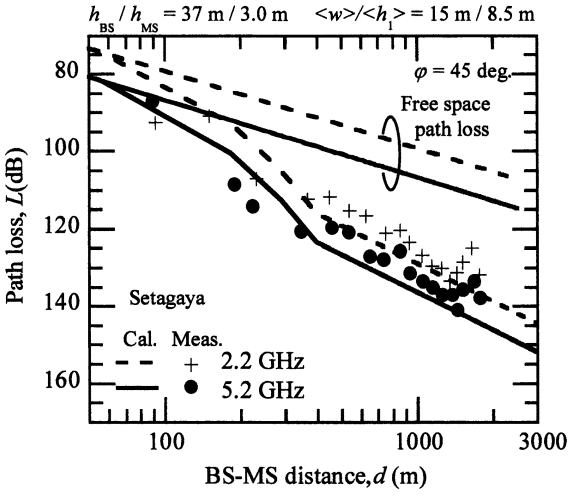

Fig. 8. Comparison with measured data (Setagaya).

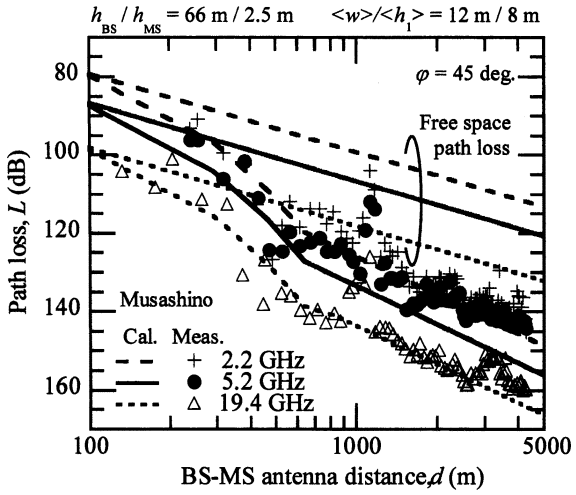

Fig. 9. Comparison with measured data (Musashino).

at 5.2 GHz, where the BS–MS antenna distance d is large, is increased. However, the computational results and the measured results agree well at 2.2 and 19.4 GHz. In particular, in both Figs. 8 and 9, the path-loss estimate is found to be accurate in the short-distance reflected wave region where the slope of the path loss changes. Hence, the effectiveness of the proposed method is confirmed.

6. Conclusions

In this paper, we have developed a path-loss model for over-rooftop propagation environments at microwave band in suburban areas, intended for application to the microwave path-loss estimation method, for which standardization is proceeding rapidly. The present model is based on the geometrical optics propagation mechanism and consists of three regions: the direct wave region, the reflected wave region, and the diffracted wave region. In this scheme, the path loss from the short-distance range, including the LOS region, to the long-distance region, including the NLOS region, can be estimated continuously. The method is considered useful for radio zone design of a system with adaptive modulation, study of interference consideration in the short range intended for frequency sharing among different systems, and radio zone design for next-generation wireless access systems using microwave frequencies. Using the measured path loss data at 2.2, 5.2, and 19.4 GHz, the proposed model is verified and its effectiveness is confirmed.

The proposed model is expected to be useful in radio zone design for the microwave wireless access systems expected to be used increasingly in the future, and for short-range path-loss recommendation ITU-R P.1411-3,

which is considered important for interference consideration in the short range. International standardization of the present model is being promoted.

Acknowledgments. The authors thank Mr. K. Itokawa of Nippon Telegraph and Telephone East Corporation and Messrs. H. Watanabe, D. Mori, and T. Takao of NTT Advanced Technology Corporation for cooperation in the propagation experiments and data processing.

REFERENCES

1. Rec. ITU-R P.1411-2. Propagation data and prediction methods for the planning of short-range outdoor radiocommunication systems and radio local area networks in the frequency range 300 MHz to 100 GHz. ITU-R Recommendations, Volume 2003 P Series, ITU, Geneva, 2003.
2. European Cooperation in the Field of Scientific and Technical Research EURO-COST 231. Urban Transmission Loss Models for Mobile Radio in the 900 and 1800 MHz bands. Rev.2, The Hague, Netherlands, 1991.
3. Rec. ITU-R P.1411-3. Propagation data and prediction methods for the planning of short-range outdoor radiocommunication systems and radio local area networks in the frequency range 300 MHz to 100 GHz. ITU-R Recommendations, Volume 2005 P Series, ITU, Geneva, 2005.
4. Kita N, Uwano S, Sato A, Umehira M. A path loss model in residential areas based on measurement studied using a 5.2-GHz/2.2-GHz dual band antenna. IEICE Trans Commun 2001;E84-B:368–376.
5. Oda Y, Tsuchihashi R, Tsunekawa K, Hata M. Measured path loss and multipath propagation characteristics in UHF and microwave frequency bands for urban mobile communications. Proc IEEE Veh Tech Conf 2001;1:337–341.
6. Sakawa K, Masui H, Ishii M, Shimizu H, Kobayashi T. Non line-of-sight microwave propagation characteristics for personal communications with high-tier base station antenna. IEICE Trans Fundam 2002;E85-A:1569–1577.
7. Kitao K, Ichitsubo S. Path loss prediction formula for microcell in 400 MHz to 8 GHz band. Electron Lett 2004;40:685–687.
8. Andersen JB, Rappaport TS, Yoshida S. Propagation measurements and models for wireless communications channels. IEEE Commun Mag 1995;33:42–49.
9. Erceg V, Greenstein LJ, Tjandra SY, Parkoff SR, Gupta A, Kulic B. An empirically based path loss model for wireless channels in suburban environments. IEEE J Sel Areas Commun 1999;17:1205–1211.
10. Batariere MD, Blankenship TK, Kepler JF, Krauss TP, Lisica I, Mukthavaram S, Porter JW, Thomas TA, Vook FW. Wideband MIMO mobile impulse response measurements at 3.7 GHz. IEEE Veh Tech Conf 2002;1:6–10.
11. McNamara DA, Pistorius CWI, Malherbe JAG. Introduction to the uniform geometrical theory of diffraction. Artech House; 1990.
12. Lott M, Fifield Y, Evans D, Hulyalkar S. Radio channel characteristics for typical environments at 5.2 GHz. ACTS Mobile Communication Summit, p 252–257, Aalborg, Denmark, 1997.
13. Bramley EN, Cherry SM. Investigation of microwave scattering by tall buildings. Proc IEE 1973;120:833–842.
14. Walfisch J, Bertoni HL. A theoretical model of UHF propagation in urban environments. IEEE Trans Antennas Propag 1988;36:1788–1797.

AUTHORS (from left to right)

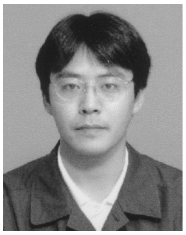

Naoki Kita (member) graduated from the Department of Electronic Systems Engineering, Tokyo Metropolitan Institute of Technology, in 1994, completed the M.S. program at Tokyo Institute of Technology in 1996, and joined NTT. Since then, he has been engaged in research on radio zone design for high-speed wireless access systems and radio propagation technologies. He is now a research engineer at NTT Access Network Service Systems Laboratories. He received the Young Researcher's Award from IEICE in 2001. He is a member of IEEE.

Wataru Yamada (member) graduated from the Department of Electronic Engineering, Hokkaido University, in 2000, completed the M.S. program in 2002, and joined NTT. Since then, he has been engaged in research on radio propagation techniques for high-speed wireless access systems. He is a member of IEEE.

Akio Sato (member) graduated from the Department of Electrical Engineering, Kyushu University, in 1979, completed the M.S. program in 1981, and joined Nippon Telegraph and Telephone Public Corporation (now NTT). Since then, he has been engaged in research and development related to 26-GHz wireless subscriber systems, propagation characteristics for microwave long-haul relay system, propagation characteristics for wireless access systems. In 2004, he became a professor at Tokyo University of Technology. He holds a Ph.D. degree, and is a member of IEEE.